

Rayleigh anomaly-surface plasmon polariton resonances in palladium and gold subwavelength hole arrays

H. Gao,¹ J. M. McMahon,^{2,3} M. H. Lee,² J. Henzie,²
S. K. Gray,³ G. C. Schatz,² and T. W. Odom^{1,2*}

¹Department of Materials Science and Engineering, Northwestern University, Evanston, Illinois 60208, USA

²Department of Chemistry, Northwestern University, Evanston, Illinois 60208, USA

³Chemistry Division and Center for Nanoscale Materials, Argonne National Laboratory, Argonne, Illinois 60439, USA

*Corresponding author: tdom@northwestern.edu

Abstract: Surface plasmon polaritons (SPPs) and Rayleigh anomalies (RAs) are two characteristic phenomena exhibited by periodic grating structures made of plasmonic materials. For Au subwavelength hole arrays, SPPs and RAs from opposite sides of the film can interact under certain conditions to produce highly intense, narrow spectral features called RA-SPP resonances. This paper reports how RA-SPP effects can be achieved in subwavelength hole arrays of Pd, a weak plasmonic material. Well-defined resonances are observed in measured and simulated optical transmission spectra with RA-SPP peaks as narrow as 45 nm (FWHM). Dispersion diagrams compiled from angle-resolved spectra show that RA-SPP resonances in Pd hole arrays shift in wavelength but do not decrease significantly in amplitude as the excitation angle is increased, in contrast with RA-SPP peaks in Au hole arrays. The apparent generality of the RA-SPP effect enables a novel route to optimize resonances in non-traditional plasmonic media.

© 2009 Optical Society of America

OCIS codes: (240.6680) Surface plasmons; (050.6624) Subwavelength structures; (260.3910) Metal optics; (160.4236) Nanomaterials; (280.4788) Optical sensing and sensors; (290.3030) Index measurements

References and links

1. P. B. Johnson and R. W. Christy, "Optical Constants of the Noble Metals," *Phys. Rev. B* **6**, 4370 (1972).
2. P. B. Johnson and R. W. Christy, "Optical constants of transition metals: Ti, V, Cr, Mn, Fe, Co, Ni, and Pd," *Phys. Rev. B* **9**, 5056 - 5070 (1974).
3. H. Gao, J. Henzie, M. H. Lee, and T. W. Odom, "Screening plasmonic materials using pyramidal gratings," *Proc. Natl. Acad. Sci.* **105**, 20146–20151 (2008).
4. J. Valentine, S. Zhang, T. Zentgraf, E. Ulin-Avila, D. A. Genov, G. Bartal, and X. Zhang, "Three Dimensional Optical Metamaterial Exhibiting Negative Refractive Index," *Nature* **455**, 376 (2008).
5. D. Pacifici, H. J. Lezec, and H. A. Atwater, "All-optical modulation by plasmonic excitation of CdSe quantum dots," *Nature Photon.* **1**, 402-406 (2007).
6. M. E. Stewart, C. R. Anderton, L. B. Thompson, J. Maria, S. K. Gray, J. A. Rogers, and R. G. Nuzzo, "Nanostructured Plasmonic Sensors," *Chem. Rev.* **108**, 494-521 (2008).
7. R. Gordon, D. Sinton, K. L. Kavanagh, and A. G. Brolo, "A new generation of sensors based on extraordinary optical transmission," *Accts. Chem. Res.* **41**, 1049-1057 (2008).
8. H. Gao, J. Henzie, and T. W. Odom, "Direct Evidence for Surface Plasmon-Mediated Enhanced Light Transmission through Metallic Nanohole Arrays," *Nano. Lett.* **6**, 2104-2107 (2006).
9. J. Henzie, M. H. Lee, and T. W. Odom, "Multiscale Patterning of Plasmonic Metamaterials," *Nature Nanotech.* **2**, 549-554 (2007).
10. J. M. McMahon, J. Henzie, T. W. Odom, G. C. Schatz, and S. K. Gray, "Tailoring the Sensing Capabilities of Nanohole Arrays in Gold Films with Rayleigh Anomaly-Surface Plasmon Polaritons," *Opt. Express* **15**, 18119-18129 (2007).

11. W. L. Barnes, A. W. Murray, J. Dintinger, E. Devaux, H. J. Lezec, and T. W. Ebbesen, "Surface plasmon polaritons and their role in the enhanced transmission of light through periodic arrays of sub-wavelength holes in a metal film," *Phys. Rev. Lett.* **92**, 107401 (2004).
12. D. Sarid, "Long-Range Surface-Plasma Waves on Very Thin Metal Films," *Phys. Rev. Lett.* **47**, 1927 - 1930 (1981).
13. L. Martin-Moreno, F. J. Garcia-Vidal, H. J. Lezec, K. M. Pellerin, T. Thio, J. B. Pendry, and T. W. Ebbesen, "Theory of Extraordinary Optical Transmission through Subwavelength Hole Arrays," *Phys. Rev. Lett.* **86**, 1114 - 1117 (2001).
14. G. C. Schatz, J. M. McMahon, and S. K. Gray, "Tailoring the parameters of nanohole arrays in gold films for sensing applications," *Proc. SPIE* **6641**, 664103/664101 - 664103/664108 (2007).
15. C. Genet, M. P. v. Exter, and J. P. Woerdman, "Fano-type interpretation of red shifts and red tails in hole array transmission spectra," *Opt. Commun.* **225**, 331 - 336 (2003).
16. S.-H. Chang, S. K. Gray, and G. C. Schatz, "Surface plasmon generation and light transmission by isolated nanoholes and arrays of nanoholes in thin metal films," *Opt. Express* **13**, 3150-3165 (2005).
17. O. M. Piciu, M. W. Docter, M. C. v. d. Krogt, Y. Garini, I. T. Young, P. M. Sarro, and A. Bossche, "Fabrication and optical characterization of nano-hole arrays in gold and gold/palladium films on glass" *Proc. Inst. Mech. Engin. Part N: J. Nanoengin. Nanosyst.* **221**, 107-114 (2007).
18. J. Steele, C. Moran, C. Aguirre, A. Lee, and N. Halas, "Metallodielectric gratings with subwavelength slots: Optical properties," *Phys. Rev. B* **68**, 205103 (2003).
19. R. C. Vehse, E. T. Arakawa, and M. W. Williams, "Optical and Photoemissive Properties of Palladium in the Vacuum Ultraviolet Spectral Region," *Phys. Rev. B* **1**, 517 - 522 (1970).

Surface plasmon polaritons (SPPs) are collective oscillations of conduction electrons trapped at metal-dielectric interfaces. Because the real part of the electric permittivity ϵ' (complex permittivity of the metal $\epsilon_m = \epsilon' + i\epsilon''$) changes sign at the metal-dielectric interface, evanescent SPP fields are highly concentrated at the boundary. For noble metals such as Au and Ag, the small imaginary part of the dielectric constant ($\epsilon'' \ll |\epsilon'|$) at visible wavelengths [1] results in small ohmic energy dissipation, which gives rise to narrow plasmon resonance. In contrast, metals such as Pd have relatively large ϵ'' values [2] and are categorized as weak plasmonic materials [3]. Manipulating confined electromagnetic fields and tailoring the SPP resonances in different plasmonic media are crucial for developing negative index materials [4], nanoscale optical switches [5], and label-free chemical/biological sensors [6, 7]. To improve the performance of plasmonic devices, significant effort has been devoted toward optimizing the quality of SPPs (e.g. producing intense and narrow resonances) as well as their tunability. For example, we have demonstrated that well-defined SPP-Bloch wave (SPP-BW) modes can be achieved in microscale arrays of nanoholes [8] and nanohole patches [9], and that unexpected sharp and strong Rayleigh anomaly-SPP (RA-SPP) resonances can be formed in Au subwavelength hole arrays [10].

When light is incident on a 2D square array of subwavelength holes with lattice constant a_0 , photons can gain additional momentum in integer multiples of $|\mathbf{G}_x| = |\mathbf{G}_y| = 2\pi/a_0$, and SPP-BW modes are generated under the Bragg coupling condition [11]

$$\text{Re} \left[\frac{\omega}{c} \sqrt{\frac{\epsilon_m \epsilon_d}{\epsilon_m + \epsilon_d}} \right] = |\mathbf{k}_0 \sin \theta + i\mathbf{G}_x + j\mathbf{G}_y| \quad (1)$$

where ω , c , and \mathbf{k}_0 are the angular frequency, speed, and momentum of free-space light, and ϵ_d is the relative permittivity of the adjacent dielectric material, which can be expressed in terms of refractive index ($n^2 = \epsilon_d$) for non-absorbing materials. Integer index pairs (i, j) denote specific SPP modes, and θ is the excitation angle. If the metal hole arrays are sandwiched between a dielectric substrate (*sub*) and superstrate (*sup*), SPP-BWs excited at the metal-*sub* interface can efficiently tunnel through the nanoholes to the metal-*sup* interface, where they are scattered back into plane waves, which then contribute to the overall light transmission (i.e. enhanced optical transmission, or EOT). The coupling of SPPs on opposite sides of the metal film can also occur [12, 13], and we found that coupled SPPs on Au films supported on glass [10] can produce a lower energy symmetric mode and a higher energy antisymmetric mode.

Besides SPP waves, another optical phenomenon is the RA (sometimes referred to as a Wood anomaly or Rayleigh-Wood anomaly), which is associated with light diffracted parallel to the grating surface. RAs occur when

$$\frac{\omega}{c}\sqrt{\varepsilon_d} = |\mathbf{k}_0 \sin \theta + i\mathbf{G}_x + j\mathbf{G}_y| \quad (2)$$

which is related to ε_d and the grating pitch but not the grating material (i.e., no dependence on ε_m). The wavelength of the RA occurs at the onset of the (i, j) diffraction order, above which free-space light diffraction is forbidden in the order. Although a RA is a non-resonant spectral feature, the interplay between RAs and SPPs on opposite sides of the metal film (the RA-SPP effect) can lead to narrower spectral features [10] and sometimes a higher EOT. Unlike the coupling between SPPs, we have demonstrated that the coupling between RAs and SPPs only occurs for a range of film thicknesses [14].

Here, we investigated the optical properties of Pd subwavelength hole arrays and observed well-defined SPP resonances associated with EOT. The most narrow and intense resonances, however, were RA-SPP resonances; the broad, long wavelength peak obscured SPP coupling on opposite sides of the Pd film. Importantly, the RA-SPP resonances in Pd hole arrays could be tuned over a large spectral range either by changing the surrounding dielectric environment or the excitation conditions. Different from those observed in Au hole arrays, the RA-SPP features in Pd occurred at high angles of excitation without significant changes in peak amplitude or peak width.

Large-area ($> 1 \text{ in}^2$) Pd subwavelength hole arrays were fabricated by a combination of SIL and PEEL techniques [9]. SIL was used to generate square arrays of photoresist posts

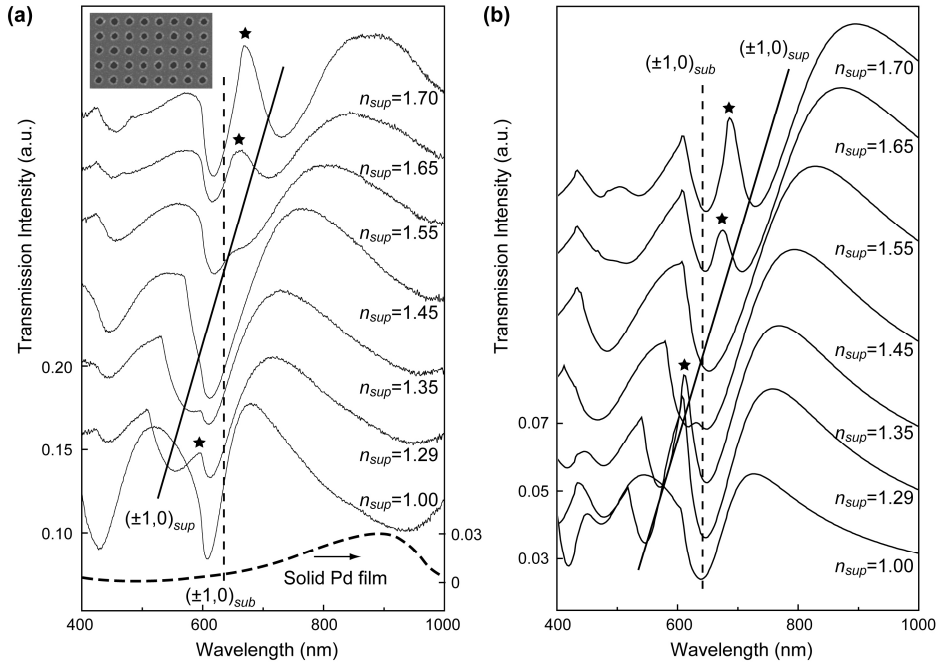


Fig. 1. Zero-order transmission spectra of Pd subwavelength hole arrays under normal incidence excitation. (a) Measured and (b) FDTD calculated spectra are in excellent agreement, and the position of the SPP minima are in good agreement with Eq. (1) (solid and dashed lines). Transmission through a 55-nm solid Pd film is included as a reference. RA-SPP resonances are indicated by \star . Inset of (a) is an SEM image of 400-nm pitch Pd hole arrays.

(diameter $d = 160 \text{ nm}$, pitch $a_0 = 400 \text{ nm}$) on a Si (100) substrate, which were then transferred into subwavelength hole arrays with film thickness $t = 55 \text{ nm}$ using PEEL (Fig. 1(a), inset).

Zero-order transmission spectra were obtained using a home-built rotational stage. Pd hole arrays sandwiched between glass substrates and oil superstrates were illuminated with collimated white light (Thorlabs OSL1 180-W fiber coupled halogen lamp, beam diameter ≈ 2 mm, divergence angle $< 0.4^\circ$). The transmitted light was collected by a fiber coupler through a 0.5-mm iris located about 20 cm behind the sample. Figure 1(a) shows that Pd subwavelength hole arrays in air ($n_{sub} = 1.523$, $n_{sup} = 1.00$) exhibit transmission intensities up to 18% at 665 nm. The transmission through a 55-nm thick solid Pd film was very weak at most wavelengths except for a broad peak around 900 nm with maximum intensity of 3% (Fig. 1(a), dashed line). Considering that the geometric open area of the hole array films was 12%, we found that EOT was obtained in this relatively weak plasmonic metal. The EOT observed in these Pd hole arrays was found to be closely related to the excitation of SPP-BW modes.

As predicted by Eq. (1), maxima and minima in the transmission spectra were red-shifted with increasing n_{sup} . The resonance features in the transmission spectra exhibited a Fano profile [15], corresponding to a sharp minimum followed by an adjacent maximum [16]. The minima in the experimental spectra were closer to the predictions of Eq. (1). Zero-order transmission spectra of Pd hole arrays under normal incidence were also simulated using the finite-difference time-domain (FDTD) method [10] with $n_{sup} = 1.00$ to 1.70 (Fig. 1(b)). The calculated spectral features and experimental data showed excellent agreement regarding the frequencies of resonances. Slight differences in transmission amplitude were most likely because of minor yet unavoidable imperfections in the Pd samples (such as variations in hole size, film thickness, and surface roughness).

As n_{sup} was increased past an index value of 1.55, the $(\pm 1, 0)_{sup}$ RA wavelength approached the $(\pm 1, 0)_{sub}$ SPP mode, and a distinct peak as narrow as 45 nm appeared at 670 nm (Fig. 1, ★). Because $|\epsilon'_{Pd}| > |\epsilon'_{Au}|$ ($\epsilon'_{Pd} = -16.7$, $\epsilon'_{Au} = -14.4$ at 670 nm), plasmon resonances on Pd occurred at bluer wavelengths, and the RA-SPP peak was also blue-shifted by ca. 20 nm. When n_{sup} approached 1.29, the RA-SPP resonances occurred as $(\pm 1, 0)_{sup}$ SPPs overlapped with $(\pm 1, 0)_{sub}$ RAs. Because Pd films attenuate the propagation of SPP waves more strongly than Au at optical wavelengths, the RA-SPP peak at 670 nm from Pd hole arrays was broader and less intense compared to the same RA-SPP mode on Au at 690 nm (FWHM = 34 nm) [9]. However, these RA-SPP spectral features are more well-defined and much narrower compared to previous reports that did not observe strong resonances from Pd

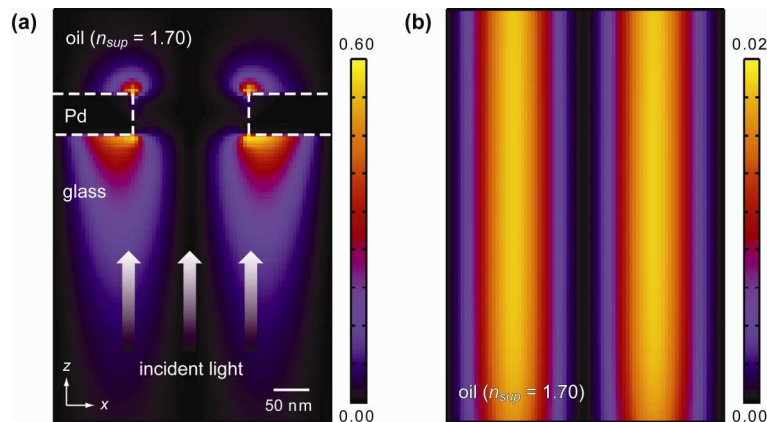


Fig. 2. Simulated electromagnetic field distributions ($|E_x|^2$) at a RA-SPP minimum ($\lambda = 628$ nm). (a) SPPs are visible on both sides of the Pd hole array film, where n_{sub} (glass) = 1.52, and n_{sup} (oil) = 1.70. (b) RA at $z = 200$ nm above the film, where SPPs have significantly decayed.

substrates [17]. Furthermore, because ϵ''_{Pd} becomes *smaller* with decreasing wavelength (a somewhat unusual feature) [2], Pd becomes more free electron-like at shorter wavelengths, and the plasmon resonances therefore can be very distinct in the blue region of the visible spectrum.

The strongest RA-SPP peak for $n_{\text{sup}} > 1.55$ occurred at a wavelength that was slightly longer than the RA condition at the Pd-*sub* interface but shorter than the SPP resonance at the Pd-*sup* interface. In this case, first order diffraction is a virtual process, which means that SPP excitation associated with the bottom of the film can temporarily populate the virtual diffraction channel before ultimately scattering to the zero-order channel. This pathway operates in parallel with normal zero-order scattering to enhance transmission. When the wavelength is reduced further to allow first order diffraction, scattering to the zero-order channel stops, leading to a sharp cutoff in the RA-SPP peak on the short wavelength side. Therefore, sharp features in the transmission spectra can be observed even though Pd has a large ϵ'' at these wavelengths. An analogous process happens for $n_{\text{sup}} < 1.55$ except that the roles of the Pd-*sup* and Pd-*sub* interfaces are reversed.

Strong variations in the transmission amplitude from the RA-SPP effect were observed in FDTD calculations near 606 nm when $n_{\text{sup}} = 1.293$ and near 685 nm when $n_{\text{sup}} = 1.70$ (Fig. 1(b), ★). To verify coupling between the $(\pm 1, 0)_{\text{sub}}$ SPP and the $(\pm 1, 0)_{\text{sup}}$ RA, we plotted the

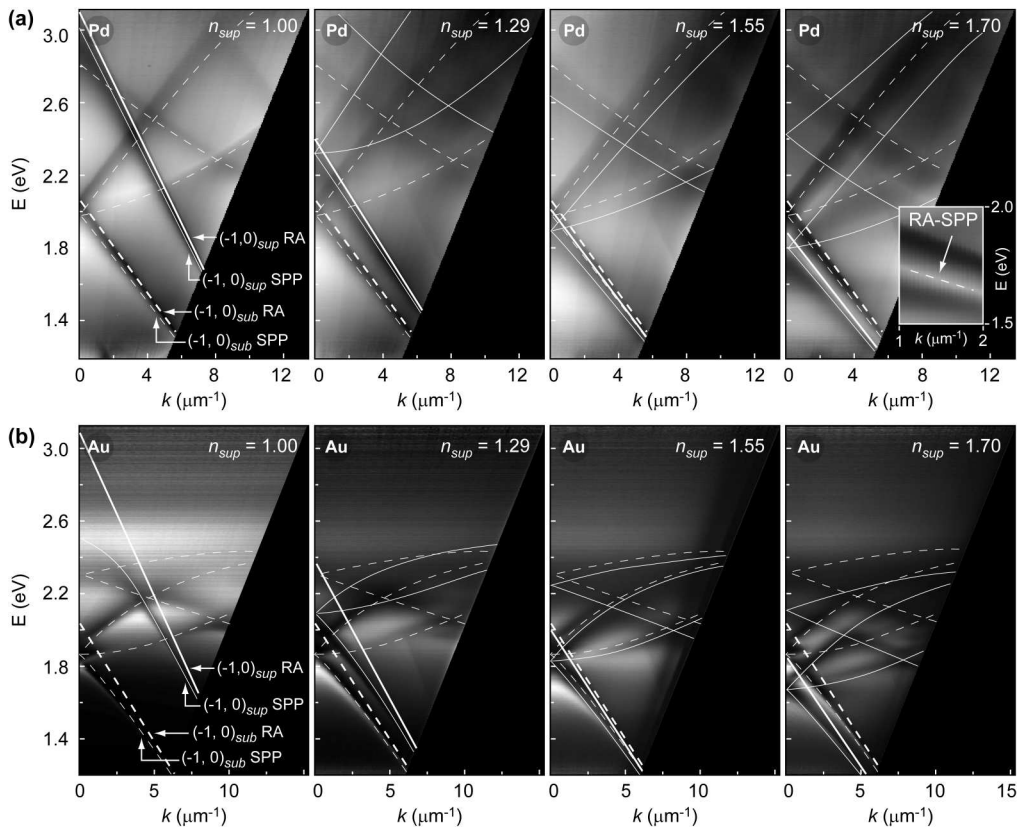


Fig. 3. Dispersion diagrams of (a) Pd and (b) Au subwavelength hole arrays. Measured spectra agreed with predicted SPP-BW modes (thin lines) at the metal-*sup* (thin, solid lines) and the metal-*sub* (thin, dashed lines). Calculated RA bands (thick lines) are also displayed. Inset in (a) is a zoom-in view of the RA-SPP band in Pd hole arrays when $n_{\text{sup}} = 1.70$. Note that $n_{\text{sup}} = 1.70$ results from Eqs. (1) and (2) with $(i, j) = (-1, 0)$ for both the RA and SPP. Hence, because the RA and SPP bands completely overlap, we have called this feature a RA-SPP band.

Fourier transformed field intensity $|E_z|^2$ at 628 nm for $n_{sup} = 1.70$, near the minimum in the zero-order transmission spectrum associated with the RA-SPP peak (Fig. 2). Figure 2(a) shows that the SPP has greatest intensity at the Pd-*sub* interface, but intensity was also noticeable on the superstrate side. The RA is also present along with the SPPs but cannot be resolved because of its low intensity relative to the SPP. Figure 2(b) shows the field at $z > 200$ nm above the hole where the SPP fields have significantly decayed and the electromagnetic characteristics of the RA are evident (i.e., a propagating plane wave with infinite extent) [18].

The identification of specific SPP modes from normal-incidence spectra can be difficult when there are degeneracies or when multiple broad and weak maxima/minima overlap with each other. Such challenges can be overcome using angle-resolved transmission spectroscopy because SPP modes that are degenerate when $\theta = 0^\circ$ ($k_x = 0$) will split at other angles ($k_x \neq 0$) (Eq. (1)). Taking advantage of our large-area samples, we mapped out the SPP band structures of Pd hole arrays out to high angles ($\theta = 70^\circ$) and converted them into E - k_x dispersion diagrams (Fig. 3), where E is the photon energy, k_x is the in-plane wavevector of the incident light in air. The grayscale represents the transmission intensity. Two sets of plasmonic (SPP) and photonic (RA) bands were observed at the Pd-*sub* interface (Fig. 3, dashed lines from Eq. (1) and (2)) and the Pd-*sup* interface (Fig. 3, solid lines). As expected, when n_{sup} increased, the Pd-*sub* modes did not change while the Pd-*sup* modes shifted to lower E . Good agreement was found between the predicted modes and the dispersion diagrams, which verified the spectral features originated from SPP-BWs.

The dispersion diagrams of Pd hole arrays show distinct differences from Au hole arrays (Fig. 3(b)): (1) Pd SPP resonances are observed at shorter wavelengths because the interband transitions of Pd occur near 3.6 eV (ca. 344 nm) [19], but Au plasmon resonances are obscured by the intrinsic interband transitions around 2.5 eV (ca. 500 nm) [10]; (2) the $(-1, 0)$ SPP band of the Pd hole arrays is nearly linear and parallel to the RA line because ϵ'_{Pd} changes more slowly than ϵ'_{Au} throughout the optical regime [1, 2], whereas the SPP bands of Au hole arrays exhibit slopes different from the RA curves; and (3) the bright RA-SPP bands

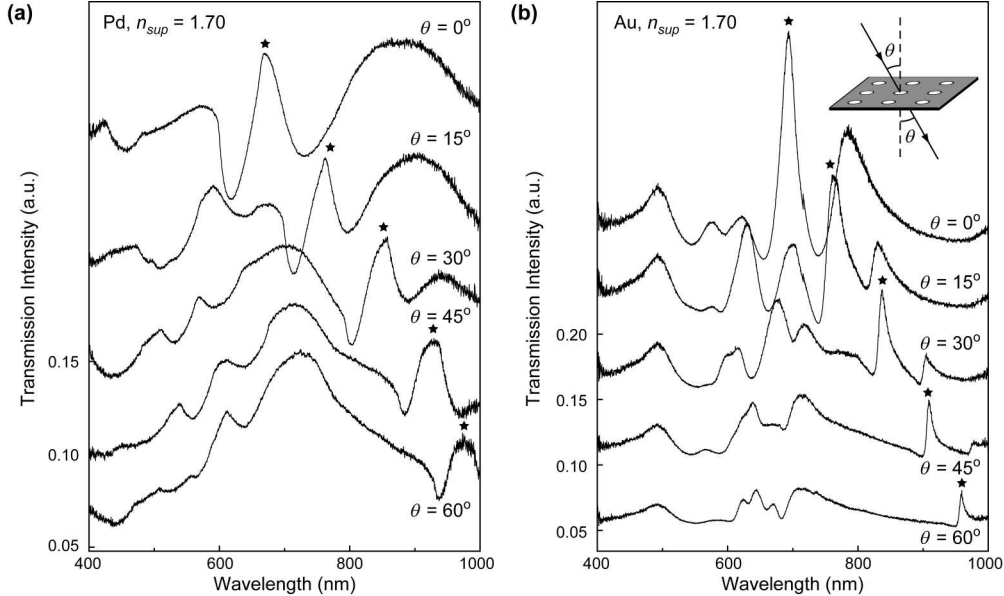


Fig. 4. Angle-resolved transmission spectra of (a) Pd and (b) Au subwavelength hole arrays with $n_{sup} = 1.70$. The RA-SPP resonance (★) in Pd shifted with θ but did not change much in amplitude and peak width, whereas the intensity of the RA-SPP peak in Au hole arrays dramatically decreased with increasing θ .

of the Pd hole arrays remain intense with increased k_x (Fig. 3(a), $n_{sup} = 1.70$, inset), while the equivalent band in Au becomes weak at large wavevectors (Fig. 3(b), $n_{sup} = 1.70$).

Since both SPPs and RAs are angle dependent, RA-SPP peaks also shift with incident angle. The required condition for the RA-SPP effect—overlap between the $(-1, 0)_{sub}$ SPP mode and the $(-1, 0)_{sup}$ RA mode—in Pd occurred not only at normal incidence ($\theta = 0^\circ$) but also out to large angles *without* changes in n_{sup} because SPP and RA bands have similar slopes as function of θ . Figure 4(a) shows that the RA-SPP peak of Pd hole arrays exhibits nearly the same amplitude and FWHM at angles from 0° to 60° . In contrast, the amplitude of the RA-SPP peak of Au hole arrays decreases dramatically with increased θ when $n_{sup} = 1.70$ (Fig. 4(b)) because the $(-1, 0)_{sub}$ SPP band deviates significantly from the $(-1, 0)_{sup}$ RA one at large angles. Therefore, changing the excitation angle presents another effective approach to tune RA-SPP resonances to desirable wavelengths in Pd without compromising the spectral quality.

In summary, we have shown that Pd subwavelength hole arrays exhibit both EOT and RA-SPP resonances that were previously observed only in Au hole arrays. There are at least three important implications of this work: (1) RA-SPP resonances are a general effect that may be observed in plasmonic materials under the proper conditions; (2) hole arrays or related structures created from weak plasmonic materials offer new prospects for constructing plasmonic components; and (3) the design of SPP-based sensors and surface-enhanced Raman scattering substrates that require short wavelengths for efficient excitation can be improved.

Acknowledgments

This work was supported by the National Science Foundation (NSF) under DMR-0705741, the NSF-NSEC (EEC-0647560), the NSF-MRSEC (DMR-0520513), and the DOE BES (DE-AC02-06CH11357). This work made use of the NSERC computation facilities, supported by DOE, and the NUANCE Center facilities, supported by NSF-MRSEC, NSF-NSEC and the Keck Foundation.